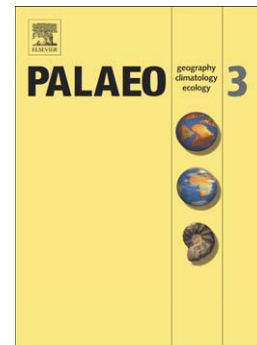# Accepted Manuscript

High-precision U-Th dating of storm-transported coral blocks on Frankland Islands, northern Great Barrier Reef, Australia

En-tao Liu, Jian-xin Zhao, Tara R. Clark, Yue-xing Feng, Nicole D. Leonard, Hannah Markham, John M. Pandolfi

Please cite this article as: Liu, En-tao, Zhao, Jian-xin, Clark, Tara R., Feng, Yuexing, Leonard, Nicole D., Markham, Hannah, Pandolfi, John M., High-precision U-Th dating of storm-transported coral blocks on Frankland Islands, northern Great Barrier Reef, Australia, *Palaeogeography, Palaeoclimatology, Palaeoecology* (2014), doi: 10.1016/j.palaeo.2014.08.017

High-precision U-Th dating of storm-transported coral blocks on Frankland Islands,

northern Great Barrier Reef, Australia

En-tao Liu[a.b*1], Jian-xin Zhao[b*], Tara R. Clark[b], Yue-xing Feng[a,b], Nicole D. Leonard[b],

Hannah Markham[c], John M. Pandolfi[c]

a. Faculty of Earth Resources, China University of Geosciences, Wuhan 430074,

China

b. Radiogenic Isotope Facility, School of Earth Sciences, The University of

Queensland, Brisbane, Qld 4072, Australia

c. Centre for Marine Science, School of Biological Sciences, the University of

Queensland, Brisbane Qld 4072, Australia

---

*Corresponding author: Radiogenic Isotope Facility, School of Earth Sciences,

The University of Queensland, Brisbane, Qld 4072, Australia. Tel: +61 7 33469753;

fax: +61 7 33658530; E-mail addresses: l.entao2012@gmail.com (E.T. Liu),

j.zhao@uq.edu.au (J.-X. Zhao)

Abstract: High-energy storm-transported coral blocks are widespread on the reef flats of the Great Barrier Reef (GBR), Australia, and have the potential to be used as proxies for reconstructing past storm/cyclone events prior to historical or instrumental records. In this study, samples from 42 individual transported coral blocks were collected from the inshore Frankland Islands, northern GBR for high-precision MC-ICPMS U-Th dating with their surface mortality ages recording the timing of individual storms or cyclones responsible for their uplift from their original growth position. The dated mortality ages were found to match well with known historical storm/cyclone events in the last century, with 80% of them falling within episodes of increased storm activity (1910-1915, 1945-1950, 1955-1960, 1975-1990, 1995-2000AD) captured by instrumental/historic records, confirming that transported coral blocks on inshore reefs can be used as proxies for past storm/cyclone occurrences. Using this approach, this study also identified 17 additional storm/cyclone events that occurred before European settlement in the 1850's, including three oldest events at 758.4±3.7, 777.9±4.9, and 985.2±4.8 AD, respectively. Our results, despite still preliminary, suggest that the storm/cyclone activity in this region tends to broadly correlate with the positive modes of the Pacific Decadal Oscillation (PDO) during the last millennium. In addition, there appears to be a decreasing age trend from the shore to the reef edge (from 758.4±3.7AD to 1988.3±1.6 AD), which can be attributed to sea-level fall and/or reef/island progradation over the last 2000 years.

Key words: Storm activity; U-Th dating; Coral blocks; Great Barrier Reef

1. Introduction

In tropical regions, strong storm events such as cyclones, hurricanes, typhoons and episodes of strong winds rank as one of the main threats to both economics and human life of any natural hazard after drought (Connell et al., 1997; Nott and Hayne, 2001; Scheffers and Kelletat, 2003; Yu et al., 2004; Scheffers and Scheffers, 2006; Donnelly and Woodruff, 2007; Kleinen, 2007; Nott et al., 2007; Etienne et al., 2011; Gelfenbaum et al., 2011; McAdoo et al., 2011; Nott, 2011; Nott and Forsyth, 2012; Yu et al., 2012b; Haig et al., 2014). For example, Cyclone Gorky struck the southeast coast of Bangladesh, north of Chittagong, in April 1991, killing nearly 140,000 people (Haque and Blair, 1992). In August 2005, Hurricane Katrina caused an estimated $108 billion of damage and more than 1833 casualties, making it one of the bloodiest hurricanes to have hit the United States in history (Blake et al., 2013). Moreover, strong storm and cyclone events also have a significant impact on reef systems (Madin and Connolly, 2006; De'ath et al., 2012), contributing significantly to coral mortality and the decline of coral cover on the mid-shelf reefs of the Great Barrier Reef (GBR)(De'ath et al., 2012).

Globally tropical cyclones are predicted to increase in magnitude and frequency under an enhanced greenhouse climate (Henderson-Sellers et al., 1998; Walsh and Ryan, 2000; Nott and Hayne, 2001; Webster et al., 2005; IPCC, 2007). However, recent studies have demonstrated great regional variability on both millennial and shorter time scales (Donnelly and Woodruff, 2007; Nott et al., 2007; Nott and Forsyth, 2012). Therefore, understanding and identifying past trends and frequencies of

palaeostorms on regional scales is of great importance for predicting future community ecological disturbances and economic loss. Yet, our ability to accurately understand variability in the occurrence of palaeostorms remains limited by the short (<100 yr) instrumental record (Nott, 1997; Nott and Hayne, 2001; Nott et al., 2007; Zhao et al., 2009a; Roff et al., 2013) and insufficient field research concerning storm event reconstruction (Scheffers and Kelletat, 2003; Scheffers et al., 2009).

Strong storms with extreme effects on sedimentary transport are known to be capable of transporting large coral blocks from reef slope environments to reef flats and shore platforms (Mastronuzzi and Sansò, 2000; Goto et al., 2009; Chagué-Goff et al., 2011; Etienne et al., 2011). To this end, storm-transported coral blocks have previously been identified as useful proxies for past storm occurrences (Mastronuzzi and Sansò, 2000; Yu et al., 2004; Goto et al., 2009; Yu et al., 2012b). However, research focusing on the reconstruction of palaeostorm events using U-Th dating is relatively rare, except for a few case studies carried out on transported blocks, storm ridge rubble and lagoon sediments from reefs in off-shore settings (Yu et al., 2004; Yu et al., 2006; Zhao et al., 2009a; Scheffers et al., 2012; Yu et al., 2012b).

In this study, we present the first palaeostorm reconstruction using coral transported blocks on inshore reefs and high-precision U-Th dating techniques. Specifically, we report a new storm chronology based on high-precision U-Th dating of transported storm blocks on the Frankland Islands, northern GBR in an attempt to provide the underpinning data for correlation of known storm/cyclone events with transported block ages, and further use this correlation to determine similar events

4

back in recent geological history.

Compared to offshore areas, the study of storm records in inshore areas is more important for understanding past land-falling cyclones (Haapkylä et al., 2013) and their impact on inshore reef health. It has been demonstrated that inshore reefs in the GBR have historically been subjected to high frequency, natural disturbance events as well as significant degradation and community structure change since European settlement (DeVantier et al., 2006; Roff et al., 2013).

Moreover, compared to offshore settings, storm-transported coral blocks from high-turbidity inshore environments are usually contaminated by terrestrially-derived sediments, contributing to higher levels of non-radiogenic (or initial) ^{230}Th (e.g. Burley et al., 2012; Yu et al., 2012b; Roff et al., 2013), posing a great challenge to their reliable and precise dating. This is especially true for young corals where the contribution of non-radiogenic ^{230}Th is proportionally significantly greater. Although a bulk-Earth ^{230}Th/^{232}Th activity value of 0.82 (atomic value ~4.4 × 10^{-6}) with a large arbitrarily assigned uncertainty of ± 50-100% has been commonly assumed to correct for the non-radiogenic ^{230}Th contribution (e.g. Eisenhauer et al., 1993), the large associated uncertainty makes the age uncertainty of the corrected ^{230}Th age for young corals too large to be meaningful (see Zhao et al., 2009b). As site-specific or region-specific initial ^{230}Th/^{232}Th values for non-radiogenic ^{230}Th correction are more appropriate than the bulk-Earth value in coral ^{230}Th age calculation (Clark et al., 2012), a site-specific mean ^{230}Th/^{232}Th in the study area is needed to improve the accuracy and precision of ^{230}Th ages. Moreover, for most inshore reef corals,

5

non-radiogenic ^{230}Th is likely to be a mixture of two components each with its own isotopically distinct ^{230}Th/^{232}Th ratio: a hydrogenous (dissolved) and a detrital (particulate) component (Clark et al. 2014b). These challenges highlight a clear requirement for a site-specific non-radiogenic ^{230}Th correction method for reliable dating of young coral samples from inshore coral reefs.

Bearing the above-described challenges in mind, here we report the results of high-precision U/Th-dated storm-transported coral blocks from the Frankland Islands region and discuss their utility to reconstruct palaeostorm/cyclone events prior to instrumental monitoring. Further we discuss the importance of a site-specific non-radiogenic ^{230}Th correction method for precise and accurate U-Th age determinations of young (usually <100 years) corals samples that enable meaningful interpretation of these storm events.

2. Study site and environment

As part of the Great Barrier Reef World Heritage Area, the Frankland Islands Group comprises five continental islands surrounded by fringing reefs, located 45 km south of Cairns, and 10 km offshore from the mouth of the Russell-Mulgrave River (Fig.1). The island group includes High, Normanby, Russell, Round and Mabel Islands (Alongi et al., 2007). The surrounding waters are part of either the Great Barrier Reef Marine Park (Commonwealth) or the Great Barrier Reef Coast Marine Park (State) with complementary zoning (see

http://elibrary.gbrmpa.gov.au/jspui/bitstream/11017/846/1/site-plan-frankland-islands-2006.pdf). Normanby Island (17º12.5´S, 146º5.0´E) covers an area of 0.04 km^2, and Russell Island (17º13.5´S, 146º5.5´E), 0.12 km^2; High Island (17º09´S, 145º59.6´E), ~1.0 km^2. Normanby Island and Russell Island are located in the southeast of the Frankland Islands, ~18 km away from the mainland. High Island lies ~7.5 km northeast of the mouth of the Mulgrave-Russell Rivers, and thus highly impacted by river runoff (Alongi et al., 2007)(Fig.1).

The fringing reefs around Normanby, High and Russell Islands support a diverse assemblage of corals. Branching and tabulate *Acropora* are common, together with a variety of massive corals such as *Porites* and numerous *Faviids* and *Mussids*. The reefs were surveyed by A. Chin and T. Ayling during 1994-1995, 1998-2000 and 2001 (Chin and Ayling, 2002), and a benthic study was conducted by the Queensland Parks and Wildlife Service (QPWS) in 1999. The initial surveys in 1994 indicated that the Frankland Islands group supported rich coral communities with an average of almost 80% live coral cover (Chin and Ayling, 2002). However, subsequent surveys revealed widespread coral breakage and matrix exfoliation with many *Acropora* table corals overturned or broken across the tips. Further, there were many broken coral fragments dispersed throughout the rubble field indicating significant coral breakage from previous cyclones and storms(Chin et al., 2006). Due to differential mortality of the various coral groups in 2001, *Porites* is now the dominant coral genus on the western side of the Frankland Islands, accounting for almost 86% of hard coral cover (Chin and Ayling, 2002).

3. Sample collection and analytical methods

During field surveys in November 2012, numerous storm-transported coral blocks were found to scatter on the reef flats of the Frankland Islands. As the majority of storm blocks were located within/below the low-tide zone, they could only be sampled during the low tide window. Forty two coral block sub-samples (3 from High Island, 25 from Normanby Island and 14 from Russell Island) were randomly collected from well-preserved growth surfaces of transported coral blocks using a hammer and chisel. Out of these samples, 30 were massive corals (e.g. *Porites*, *Platygyra*, *Favia* spp.) (Fig.2 and Table 1), varying from 0.1 to 1.8m^3, with an average size of 0.6m^3. 12 were large branching colonies of *Acropora* spp. with an average size of 0.2m^3 (Table 1). Surfaces of most colonies were well-preserved without any visible sign of erosion (Fig.2).

Using a diamond blade saw, 1-2 g of aragonite material was further removed from the larger sub-sample at an area free from any obvious signs of meteoric diagenesis or surficial organics. As some of the most pristine material was cut at a few centimeters below the surface of each sample, the sampling locations was recorded (i.e. distance from the surface in cm) and latter taken away from the U-Th age to estimate the mortality age or the timing of storm/cyclone uplift of the coral blocks. Following preliminary cleaning in Mili-Q water, sub-samples of the cleanest aragonite were crushed to a 1 mm grain size using an agate mortar and pestle, then cleaned

vigorously using procedures described in detail in Clark et al. (2014a,b).

The detrital ^{230}Th/^{232}Th ratio for non-radiogenic ^{230}Th correction was calculated using the two-component isochron method described by Clark et al. (2014a,b), utilizing six samples which were selected and coeval material treated with three different pre-treatment protocols. To achieve this, each of the six coral specimens was split into three sub-samples weighing approximately 1 g each. The first set of sub-samples were set aside as untreated (with only the removal of weathered/eroded surface). The second and third sets of sub-samples were ultrasonically cleaned in Milli-Q water 4-5 times and then soaked in 15% hydrogen peroxide (H_2O_2) for at least 10 hours, rinsed and ultra-sonicated in Milli-Q water 3 times, after which the liquid was discarded. Following enhanced cleaning, the second set of sub-samples were collected without careful selection (normal cleaning), while the third set of sub-samples were then dried at ~40°C, visually inspected under a binocular microscope and only the best quality aragonitic grains selected for dating (i.e. no detritus or secondary calcite visible).

Approximately 0.15-0.35g (most ~0.15g) of each sub-sample was spiked with a ^{229}Th-^{233}U mixed tracer and dissolved in double-distilled nitric acid following the procedures described in Clark et al. (2012). After complete digestion, 5 drops of 30% H_2O_2 were added, and the sample beakers were tightly capped and placed on a hot-plate at 90°C overnight to allow for complete decomposition of residual organic matters and homogenization of tracer-sample mixed solution. Samples were then dried on a hotplate at 60°C. For young samples, especially the vigorously cleaned

third set of sub-samples for isochrons, larger sample sizes (~0.3g) were used in order to achieve higher ^{230}Th signals to improve the precision of the ^{230}Th ages. These larger samples were treated with a $Fe(OH)_2$ co-precipitated procedure to pre-concentrate U and Th. The hydroxide precipitates were re-dissolved in 0.7 ml 7 M double-distilled HNO_3 and purified using a chemical separation process similar to that described by Zhao et al. (2009b), Yu et al. (2012) and Clark et al. (2012). All samples were measured for U and Th isotopes using a Nu Plasma Multi-Collector Inductively Coupled Plasma Mass Spectrometer (MC-ICPMS) at the Radiogenic Isotope Facility (RIF), the University of Queensland, following instrumental procedures described in detail in Clark et al. (2014a,b).

After MC-ICP-MS measurements, U-Th ages were calculated using the Isoplot/Ex 3.0 program (Ludwig, 2003). Non-radiogenic ^{230}Th was corrected using a calculated ^{230}Th/^{232}Th value based on a two-component mixing equation that accounts for: 1) the proportion of terrestrially derived particulates incorporated into the skeleton either post-mortem (major) or during coral growth (minor); and 2) the hydrogenous initial ^{230}Th incorporated into the skeleton during growth (Clark et al 2014a, b). In our approach, the hydrogenous ^{230}Th/^{232}Th can be determined by measuring initial ^{230}Th/^{232}Th ratios in live-collected *Porites* colonies of known age(Cobb et al., 2003; Shen et al., 2008; Clark et al., 2012). These measured ratios are likely to closely reflect the seawater ^{230}Th/^{232}Th ratios taken up by corals at the time when they are growing. In this study, the hydrogenous ^{230}Th component was based on initial ^{230}Th/^{232}Th values obtained from live *Porites* colonies collected from central

GBR (Clark et al., 2012), and a more conservative uncertainty of ± 20% was used.

Detrital ^{230}Th/^{232}Th was determined using the ^{230}Th/^{232}Th vs ^{238}U/^{232}Th isochrons defined by multiple coeval samples with various concentrations of ^{232}Th or ^{238}U/^{232}Th ratios reflecting varying proportions of sediment contaminants present in the samples (Clark et al. 2014a,b). The ^{230}Th/^{232}Th intercept value at ^{238}U/^{232}Th=0 from the isochron should reflect the detrital ^{230}Th/^{232}Th in sediments known to influence the area where the corals were collected (Clark et al. 2014a,b). In this study, an average isochron-inferred ^{230}Th/^{232}Th value with a conservative uncertainty of 20% to account for the variability in the region (as will be described in Section 5.1) was used.

The hydrogenous and detrital ^{230}Th/^{232}Th ratios can be used in a two-component mixing model below to allow for sample-specific correction of non-radiogenic ^{230}Th (Clark et al. 2014a,b):

$$\left(\frac{^{230}Th}{^{232}Th}\right)_{mix}=\left(\left(\frac{^{232}Th_{live}}{^{232}Th_{dead}}\right)\times\left(\frac{^{230}Th}{^{232}Th}\right)_{live}\right)+\left(\left(\frac{^{232}Th_{dead}-^{232}Th_{live}}{^{232}Th_{dead}}\right)\times\left(\frac{^{230}Th}{^{232}Th}\right)_{sed}\right)$$

Where ^{232}Th$_{live}$ and (^{230}Th/^{232}Th)$_{live}$ were obtained from the average values of live-collected *Porites* in the region. (^{230}Th/^{232}Th)$_{live}$ represents the hydrogenous component, and is based on an average activity ratio of 1.08 ± 20%obtained from live-collected *Porites* from the inshore region of the GBR (Clark et al. 2012). (^{230}Th/^{232}Th)$_{sed}$ is the detrital value obtained from the above-mentioned isochron method, and ^{232}Th$_{dead}$ is the measured ^{232}Th concentration (in ppb) in the dated dead coral sample.

11

4. Dating results

The U-Th ages of 42 samples collected from storm transported coral blocks are presented in Table 1, and data for isochron calculations are shown in Table 2 and Figure 3. The U-Th data revealed uranium concentrations to be between 2.2 and 4.2 ppm, and initial $\delta^{234}U$ values within the range of 147±3‰ (Table 1 and Table 2), typical of pristine corals and modern seawater values, respectively (Robinson et al., 2004; Shen et al., 2008; Andersen et al., 2010). ^{232}Th concentrations in the ultra-cleaned samples listed in Table 1 vary from 0.04 to 2.69 ppb, with an average of 0.76 ppb. ^{232}Th levels in the sub-samples used for isochron calculations vary dramatically from 1.1 to 144 ppb, with ^{232}Th in the untreated sub-samples being up to 100 times higher than the ultra-cleaned sub-samples. Overall, ^{232}Th levels in these corals from inshore settings are significantly higher than those from off-shore settings such as those from Heron Island in the southern GBR (Yu et al., 2012) as well as southern Pacific (e.g. Burley et al., 2012), suggesting that rigorous cleaning is essential for the removal of detrital Th for high-precision U-Th dating of corals from inshore reefs.

Overall the age results indicate that all coral blocks, except for two samples collected on Normanby Island (NI-SB-H1-01, NI-SB-H1-02) and one sample collected on High Island (HI-SB-01), were transported up to the reef flat over the last millennium. Twenty-five colonies were transported onto the reef flat after 1900 AD.

For many samples, it was not possible to date the very surface of each coral block due to the presence of organics, internal bioerosion and alteration. Assuming that post-mortem erosion was minimal (Moore and Krishnaswami, 1972; Yu et al., 2004), the coral mortality age, which recorded the time of the storm/cyclone event responsible for the removal from its living site, was calculated by taking away the number of growth bands above the sampling location to the corrected ^{230}Th date (Yu et al., 2006; Clark et al., 2012). A ±0.5 yr uncertainty associated with the sampling location was added to the ^{230}Th age uncertainties as some sampling locations may be not clearly defined, and the sampling thickness of ~0.5cm is approximate to ~0.5 year of growth.

5. Discussion

5.1 Non-radiogenic ^{230}Th correction

Dating young coral samples only a few hundred years of age is challenging mainly due to: (1) extremely low radiogenic ^{230}Th in the young carbonates complicated by contributions from procedural blanks and instrumental baselines and (2) the proportionally higher initial or detrital ^{230}Th contribution resulting in a greater influence on age precisions compared to older samples (Zhao et al., 2009b).

As discussed in detail in Clark et al. (2014b), for U-Th dating of very young samples, one of the main contributors to the age uncertainty is the procedural blank from sample preparation, column chemistry and mass spectrometric measurement.

13

With our simplified column chemistry procedure and the use of ultra-pure acids, the total ^{230}Th procedural blanks in our MC-ICP-MS analytical protocol is $1.18\pm0.24\times10^{-10}$ nmol or 0.27 ± 0.05 fg (N=12) (significantly lower than that of the TIMS protocol, e.g. Clark et al., 2012, 2014a,b), contributing <0.5 yrs to the calculated ^{230}Th ages depending on both the sample weight and uranium concentration in the sample (Clark et al., 2014b). Blank contributions have been extracted from the calculation of the measured ^{230}Th/^{232}Th and ^{230}Th/^{238}U, and the corresponding uncorrected ^{230}Th ages. The procedural blanks for ^{238}U and ^{232}Th were averaged at $1.4 \pm 0.9\times10^{-5}$ nmol (3.3 ± 2.2 pg) and $3.0 \pm 1.9\times10^{-6}$ nmol (0.69 ± 0.41 pg), respectively, which is considered negligible for coral samples which generally contain ~3 ppm U.Hydrogenous ^{230}Th comes from seawater and is incorporated into the coral skeleton during growth. Detrital ^{230}Th on the other hand, may be taken into the coral skeleton in one of two ways: 1) actively in particulate forms while the coral is still alive; and 2) passively via the infiltration of fine sediments post-mortem. While most detrital particulates incorporated post-mortem can be physically removed using our rigorous cleaning procedures and careful sample vetting described above, a small amount of detrital ^{230}Th, as reflected by generally higher measured ^{232}Th in treated dead corals than in live corals of the same species, still needs to be accounted for (see Clark et al. 2014a,b). To correct for the presence of non-radiogenic ^{230}Th, ^{230}Th/^{232}Th ratios for both hydrogenous and detrital components need to be appropriately constrained. For precise and accurate dating of dead corals from the Frankland Islands region, it is important to constrain and correct for non-radiogenic hydrogenous and

14

detrital ^{230}Th sources incorporated during growth and post-mortem using the equation in Section 3. As described previously, the live *Porites* colonies collected from central GBR were determined by (Clark et al., 2012) to have a corresponding ^{230}Th/^{232}Th$_{live}$ activity ratio of 1.083 ± 0.082 (atomic value of 5.77±0.52×10^{-6}), which is very similar to the mean value of live corals from whole length of inshore GBR, and was thus considered as being suitable for the correction of the hydrogenous ^{230}Th in this study. To encompass the full range of variation, a more conservative uncertainty of 20% was used.

To estimate the detrital ^{230}Th/^{232}Th for the Frankland Islands region, we used the isochron approach. In this study, three sets of subsamples of varying ^{232}Th levels or ^{238}U/^{232}Th ratios were obtained by splitting one sample into three aliquots followed by different pre-treatment or cleaning procedures as described in Section 3. A total of 6 coral specimens were processed this way. By plotting the data of the sub-samples onto the ^{230}Th/^{232}Th vs ^{238}U/^{232}Th diagram, sub-samples for each coral specimen showed a large spread in ^{238}U/^{232}Th ratios, yielding a well-defined isochron. A total of six isochrons were obtained, each giving an intercept value on the ^{230}Th/^{232}Th axis, approximating the detrital ^{230}Th/^{232}Th in that specific coral specimen (Table 2 and Fig. 3). The six ^{230}Th/^{232}Th intercept values gave an unweighted mean of 0.64±0.11 (18%) (Fig. 3), which is similar to that previously reported for the Palm Islands region in the central GBR (Clark et al., 2014a,b)..

Using a detrital ^{230}Th/^{232}Th activity ratio [i.e. (^{230}Th/^{232}Th)$_{sed}$] of 0.64±20% and a hydrogenous ^{230}Th/^{232}Th activity ratio [i.e. (^{230}Th/^{232}Th)$_{live}$] of 1.08±20% to account

for contaminant sources of [230]Th in the coral samples, we reliably determined the timing of mortality for 42 storm transported coral colonies to have occurred between 758 ± 3.7 and 2004.4 ± 3.3 AD, with 60% of samples dated after 1900 AD (Tables 1 and 2).Thus this site-specific mean value with the expanded error is much more constrained than the conservative bulk Earth value, and is a better alternative for [230]Thcorrection for inshore reef corals in the northern GBR.

5.2 Correlation between transported storm block ages and the known storm/cyclone events

How reliable the mortality ages of the transported coral blocks are in reconstructing past storm events is largely dependent upon how close these ages match with known cyclone and storm events. Yu et al. (2012) determined that the smaller sized blocks are more likely to be transported by localized storms or strong winds, suggesting that just 65% of the dated ages match with known cyclone events affecting Heron Reef, southern GBR. Considering this, small blocks were not considered in the present study.

Using the information available from Australian Bureau of meteorology (http://www.bom.gov.au), WINDWORKER roof ventilator (http://www.windworker.com.au) and many other sources (e.g. Callaghan and Power, 2011; Yu et al., 2012), at least 73 tropical cyclones were documented to have affected the Frankland Islands or passed within 200 km of the islands between 1900 and 2010AD (Fig.4D). Based on these historic cyclone/storm events, six relatively stormy

periods (i.e. 1910-1915, 1925-1935, 1945-1950, 1955-1960, 1975-1990, 1995-2000AD) and four relatively less-stormy periods (i.e. 1900-1905, 1920-1925, 1950-1955, 2000-2005AD) were identified between 1900 AD and 2005AD (Fig.4D).

When comparing the mortality ages of the dated coral blocks dating to 1900-2010AD with the histogram of historic cyclone events occurring during the same period, it appears that the frequency distribution of these mortality ages match well with that of the historic cyclone events (especially those < 50 km from the study area), with the majority of the age data falling into the 1970-1990 period. It is also worth noting that 80% (21 out of 24 coral blocks) of the mortality ages of the last century fall within five relatively stormy periods (except for the 1930-1935 AD period), and very few samples fall within the relatively less-stormy periods (1900-1905, 1920-1925, 1950-1955, 2000-2005AD) (Fig.4D), suggesting that these transported blocks are reliable indicators of past storm events.

It is worth noting that ～15 of 24 (~60%) samples dating to the last century fall into the stormiest period (1975-1990 AD) with very few samples falling within the 1930-1935 AD stormy period. Interestingly, no mortality ages obtained in this study appear to match with Cyclone Yasi in 2011, the most intense cyclone impacting on the region for the past century (Fig.4D). This discrepancy is most likely due to sampling bias as a result of an insufficient sample size. During our multi-purpose fieldwork in November 2012, we only managed to carry out opportunistic sampling of the transported blocks during a short day-time low-tide window, with transported blocks sitting near the reef front being preferentially missed due to the rapidly rising tide.

17

Another possibility could be related to the exact distance and track of individual cyclones in the vicinity of the study area. Cyclone Yasi crossed the coast at Mission Beach in 2011, approximately 80 km south of the Frankland Islands (Perry et al., 2014), whereas Cyclone Larry of the same category with the highest wind speed of 294 km/h (Ramsay and Leslie, 2008) made landfall around Innisfail in 2006, only ~40 km south of the study area. It has been documented that the magnitude of damage is directly related to the distance from the cyclone track (GBRMPA., 2011; Perry et al., 2014). Thus, the impact of Cyclone Larry on reefs in the Frankland Islands area would have been more severe than Cyclone Yasi. In this regard, it is possible that there were fewer living coral blocks available for transportation by Cyclone Yasi in 2011, as the Frankland Islands were already subjected to high frequency disturbance events prior to Yasi, especially Cyclone Larry in 2006. Because of this, we consider it is the long-term trend and correlation, rather than short-term matching with individual cyclone events, which might be more meaningful in this study.

5.3 Correlation between coral mortality and the Pacific Decadal Oscillation (PDO) during the last millennium

The Pacific Decadal Oscillation (PDO) is a long-lived climatic phenomenon modulating ocean-atmosphere variability in the Pacific basin on multi-decadal time scales, analogous to the inter-annual El Nino-Southern Oscillation (ENSO) (Linsley et al., 2000; Viles and Goudie, 2003; Wang and Picaut, 2013). Australia's climatic variability has been shown to respond to the PDO and ENSO(Power et al., 1999;

Pezza et al., 2007; McGowan et al., 2009; Rodriguez-Ramirez et al., 2014), which has been heightened during the last major climate shift (from 1977 through to at least the mid-1990's) with a positive PDO and several ENSO events affecting climates over much of eastern Australia. Proxy records of rainfall, flood and river discharge affecting coral reefs in the GBR were found to show significant PDO and ENSO periodicity (Lough, 2007; Rodriguez-Ramirez et al., 2014).

Despite sparse data coverage, results presented here indicate that at inter-decadal timescales, the PDO poses a major influence on storm/cyclone frequency with heightened activity during the positive modes of the PDO in the last millennium (Fig. 4). Most coral mortality ages fall within the positive PDO phases (e.g. 1430-1600AD, 1725-2010AD and the most recent 1977-1995AD), and are notably absent during the pronounced negative PDO phases (e.g. 1000-1300AD, 1375-1430AD, 1600-1725AD) (Fig.4). This is consistent with the results reported by Pezza et al (2007) and Grant and Walsh (2001) that show that mean tropical cyclone formation in Australia is significantly higher during positive PDO phases than during negative PDO phases. To a lesser degree, the massive coral mortality events in the South China Sea also appear to correlate with the PDO cycles (Yu et al., 2012a), suggesting it is a common feature across the Western Pacific region.

This observation can be explained in terms of warmer conditions and increased sea surface temperatures (SST) in the tropical Western Pacific during the positive PDO phases (McGowan et al., 2009), which may enhance the likelihood of intense tropical cyclone formations (Emanuel, 2005; Webster et al., 2005; Hoyos et al., 2006).

This is consistent with observed global warming and an increased in storm frequency during the most recent positive PDO phase (1977-1995AD) resulting in intense rainfall and devastating floods in the study region (Fig.4A). However, this interpretation remains speculative until more regional data are obtained.

It is worthwhile to note that while there appears to be a significant correlation between storm frequency and positive PDO phases on a broader time-scale, the correlation between transported coral block ages and the PDO index is lacking on shorter, inter-annual scales. For instance, the mortality ages for a number of transported storm blocks fall in between 1987-1990 AD, matching with a short episode of relatively negative PDO index values (or a strong La Nina phase) within a multi-decadal positive PDO phase (1977-1995AD) (Fig. 4C). This may reflect the inter-annual variability of storm activities related to ENSO (Solow and Nicholls, 1990; Basher and Zheng, 1995; Flay and Nott, 2007; Yu et al., 2012b). Indeed, on inter-annual timescales, good correlations were found between the mortality ages of the dated coral blocks in this study and the ENSO events that occurred during the period 1950-2010AD (Fig.4E). The inter-annual peaks identified from the relative probability frequency of coral mortality ages appear to coincide with strong El Niño and La Niña events in the historical record, similar to those found in the southern GBR (e.g. Yu et al., 2012). For example, the coral-based stormy periods identified here encompass the majority (8 out of 10) of the historically strong El Niño events (1957-1958, 1965-1966, 1972-1973, 1982-1983, 1991-1992, 1997-1998) and La Niña events (1955-1956, 1973-1974,1975-1976, 1988-1989) (Fig. 4E). This is consistent

with previous work in the Australia region (Nicholls, 1984; Basher and Zheng, 1995; Callaghan and Power, 2011).

5.4 Spatial age distribution of the transported coral blocks on the reef flat

In this study, the reef flat of Normanby Island where coral production is abundant was taken as an example to illustrate the spatial age distribution of transported coral blocks (Fig. 5). A total of 16 dated coral blocks were found to have a large age range o from 758.4±3.7 AD on the island side of the reef flat to 1988.3±1.6 AD on the seaward side (Fig.5). Overall, there is a general increasing trend in the ages of storm blocks as the samples get increasingly closer to the island (i.e. farthest from the sea).

This trend is consistent with sea-level change in the past 2000 years. It has been documented that sea-level in eastern Australia progressively fell from about +1 m to its present position over the past 2000 years (Larcombe et al., 1995; Baker et al., 2001; Lewis et al., 2008; Yu and Zhao, 2010), suggesting that the progressively lowering in sea level is most likely responsible for this trend in the [230]Th age distribution. Another possible cause would be the progressive overlay of beach and intertidal deposits as a result of reef progradation. In this process, the earlier storm blocks may have been buried as the reef prograded seawards and by later-stage storm deposits.

6. Conclusions

Based on detailed field observations and high-precision MC-ICPMS U-Th dating of 42 well-preserved transported coral blocks collected from the inshore Frankland Islands, northern Great Barrier Reef (GBR), we conclude that:

(1) Mortality ages for most (over 80%) of the coral blocks dated to within the last 100 years fell in the relatively stormy periods (1910-1915, 1945-1950, 1955-1960, 1975-1990, 1995-2000AD) and very few samples fell within the relatively less stormy periods, confirming that transported coral blocks on inshore reefs can be useful as proxies for past cyclone/storm occurrences.

(2) The MC-ICPMS U-Th age dating in this study allows identification of 17 additional storm/cyclone events prior to European settlement of coastal northern Australia in the 1850's (i.e. at 758.4±3.7, 777.9±4.9, 985.2±4.8, 1450.2±3.7, 1455.3±5.2, 1530.5±3.8, 1560.6±3.6, 1580.8±3.7, 1591.2±3.3, 1725.8±3.6, 1742.2±5.1, 1751.9±5.3, 1767.2±3.6, 1769.3±4.5, 1786.3±3.5, 1816.9±5.1, 1862.2±4.1AD).

(3) Despite sparse data coverage, the results presented in this study indicate that storm/cyclone activity in the northern GBR was modulated by the multi-decadal PDO, with storms/cyclones occurring more frequently during the broadly positive phases of the PDO in the last millennium. On inter-annual timescales, there appears to be some correlation between ENSO cycles and storm/cyclone occurrences.

(4) There appears to be a decreasing age trend from shore to reef edge (from 758.4±3.7AD to 1988.3±1.6 AD) in mortality age distribution of the dated coral blocks, which can be attributed to sea-level fall and the effect of reef/island

22

progradation over the last 2000 years.

Our study also demonstrates coral samples collected from inshore/near-shore settings usually contain high ^{232}Th concentrations even after rigorous cleaning to remove sediments trapped in coral skeletons, indicative of high non-radiogenic ^{230}Th contamination. Thus correction of both hydrogenous and detrital ^{230}Th components present in the coral skeletons using a two-component mixing model was required for reliable dating of young coral samples from inshore/near-shore settings. This is in sharp to corals from off-shore settings such as Heron Island of the southern GBR (Yu et al., 2012) and Yongshu Reef of the southern South China Sea (Yu et al., 2004).

Acknowledgements

References

Alongi, D.M., Trott, L.A., Pfitzner, J., 2007. Deposition, mineralization, and storage of carbon and nitrogen in sediments of the far northern and northern Great Barrier Reef shelf. Continental Shelf Research 27, 2595-2622.

Andersen, M.B., Stirling, C.H., Zimmermann, B., Halliday, A.N., 2010. Precise determination of the open ocean ^{234}U/^{238}U composition. Geochemistry, Geophysics, Geosystems: G3 11.

Baker, R.G.V., Haworth, R.J., Flood, P.G., 2001. Inter-tidal fixed indicators of former Holocene sea levels in Australia: a summary of sites and a review of methods and models. Quaternary International 83–85, 257-273.

Basher, R.E., Zheng, X., 1995. Tropical Cyclones in the Southwest Pacific: Spatial Patterns and Relationships to Southern Oscillation and Sea Surface Temperature. Journal of Climate 8, 1249-1260.

Blake, E.S., Kimberlain, T.B., Berg, R.J., Cangialosi, J.P., Beven, J.L., 2013. AL182012 Hurricane Sandy, Tropical Cyclone Report. National Hurricane Center; 157.

Burley, D., Weisler, M.I., Zhao, J.-x., 2012. High Precision U/Th Dating of First Polynesian Settlement. Plos One 7, e48769.

Callaghan, J., Power, S.B., 2011.Variability and decline in the number of severe tropical cyclonesmaking land-fall over eastern Australia since the late nineteenthcentury. Climate Dynamics, 37 (3), 647-662.

Chagué-Goff, C., Schneider, J.-L., Goff, J.R., Dominey-Howes, D., Strotz, L., 2011. Expanding the proxy toolkit to help identify past events — Lessons from the 2004 Indian Ocean Tsunami and the 2009 South Pacific Tsunami. Earth-Science Reviews 107, 107-122.

Cheng, H., Edwards, R.L., Hoff, J., Gallup, C.D., Richards, D.A., Asmerom, Y., 2000. The half-lives of uranium-234 and thorium-230. Chemical Geology 169, 17-33.

Chin, A., Ayling, T., 2002. Disturbance and recovery cycles long-term monitoring on 'unlucky' inshore fringing reefs in the Cairns Section of the GBRMP. Reef Research 10, 5-8.

Chin, A., Davidson, J., Diaz, G. Initial survey of the impact of Tropical Cyclone Larry on reefs and islands in the Central Great Barrier Reef; 2006.

Clark, T.R., Zhao, J.-x., Feng, Y.-x., Done, T.J., Jupiter, S., Lough, J., Pandolfi, J.M., 2012. Spatial variability of initial ^{230}Th/^{232}Th in modern Porites from the inshore region of the Great Barrier Reef. Geochimica Et Cosmochimica Acta 78, 99-118.

Clark, T.R., Roff, G., Zhao, J.-x., Feng, Y.-x., Done, T.J., Pandolfi, J.M., 2014a. Testing the precision and accuracy of dating coral mortality events in the last 100 years. Quaternary Geochronology 23, 35-45.

Clark, T.R., Zhao, J.-x., Roff, G., Feng, Y.-x., Done, T.J., Nothdurft, L.D., Pandolfi, J.M., 2014b Discerning the timing and cause of historical mortality events in modern Porites from the Great Barrier Reef. Geochimica et CosmochimicaActa 138, 57-80.

Cobb, K.M., Charles, C.D., Cheng, H., Kastner, M., Edwards, R.L., 2003. U/Th-dating living and young fossil corals from the central tropical Pacific. Earth and Planetary Science Letters 210, 91-103.

Connell, J.H., Hughes, T.P., Wallace, C.C., 1997. A 30-Year Study of Coral Abundance, Recruitment, and Disturbance at Several Scales in Space and Time. Ecological Monographs 67, 461-488.

De'ath, G., Fabricius, K.E., Sweatman,H., Puotinen,M.,2012. The 27-year decline of coral cover on the Great Barrier Reef and its causes. Proceedings of the National Academy of Sciences, 109, 17995-17999.

DeVantier, L.M., De'ath, G., Turak, E., Done, T.J., Fabricius, K.E., 2006. Species richness and community structure of reef-building corals on the nearshore Great Barrier Reef. Coral Reefs 25, 329-340.

Donnelly, J.P., Woodruff, J.D., 2007. Intense hurricane activity over the past 5,000 years controlled by El Niño and the West African monsoon. Nature 447, 465-8.

Eisenhauer A., Wasserburg G. J., Chen J. H., Bonani G., Collins L.B., Zhu Z. R. and Wyrwoll K. H., 1993. Holocene sea-leveldetermination relative to the Australian continent: U/Th(TIMS) and ^{14}C (AMS) dating of coral cores from the AbrolhosIslands. Earth and Planetary Science Letters114, 529–547.

Emanuel, K., 2005. Increasing destructiveness of tropical cyclones over the past 30 years. Nature 436, 686-8.

Etienne, S., Buckley, M., Paris, R., Nandasena, A.K., Clark, K., Strotz, L., Chagué-Goff, C., Goff, J.,

Richmond, B., 2011. The use of boulders for characterising past tsunamis: Lessons from the 2004 Indian Ocean and 2009 South Pacific tsunamis. Earth-Science Reviews 107, 76-90.

Flay, S., Nott, J., 2007. Effect of ENSO on Queensland seasonal landfalling tropical cyclone activity. International Journal of Climatology 27, 1327-1334.

GBRMPA(Great Barrier Reef Marine Park Authority), 2011. Impacts of tropical cyclone Yasi on the Great Barrier Reef: A report on the findings of a rapid ecological impact assessment, July 2011. Townsville: Great Barrier Reef Marine Park Authority. 21 p.

Gelfenbaum, G., Apotsos, A., Stevens, A.W., Jaffe, B., 2011. Effects of fringing reefs on tsunami inundation: American Samoa. Earth-Science Reviews 107, 12-22.

Goto, K., Okada, K., Imamura, F., 2009. Characteristics and hydrodynamics of boulders transported by storm waves at Kudaka Island, Japan. Marine Geology 262, 14-24.

Grant, A., Walsj, K., 2001.Interdecadal variability in north-east Australian tropical cyclone formation. Atmospheric Science Letters 2(1-4), 9-17.

Haapkylä, J., Melbourne-Thomas, J., Flavell, M., Willis, B.L., 2013. Disease outbreaks, bleaching and a cyclone drive changes in coral assemblages on an inshore reef of the Great Barrier Reef. Coral Reefs 32, 815-824.

Haig, J., Nott, J., Reichart, G.J., 2014. Australian tropical cyclone activity lower than at any time over the past 550-1,500 years. Nature 505, 667-671.

Haque, C.E., Blair, D., 1992. Vulnerability to Tropical Cyclones: Evidence from the April 1991 Cyclone in Coastal Bangladesh. Disasters 16, 217-229.

Henderson-Sellers, A., Zhang, H., Berz, G., Emanuel, K., et al., 1998. Tropical cyclones and global climate change: A post-IPCC assessment. Bulletin of the American Meteorological Society 79, 19-38.

Hoyos, C.D., Agudelo, P.A., Webster, P.J., Curry, J.A., 2006. Deconvolution of the Factors Contributing to the Increase in Global Hurricane Intensity. Science 312, 94-97.

IPCC, Climate Change 2007: impacts, adaptation and vulnerability : working group II contribution to the Fourth Assessment Report of the IPCC. Cambridge University Press: Cambridge and New York, 2007; pp. 1-976.

Kleinen, J., 2007. Historical perspectives on typhoons and tropical storms in the natural and socio-economic system of Nam Dinh (Vietnam). Journal of Asian Earth Sciences 29, 523-531.

Larcombe, P., Carter, R.M., Dye, J., Gagan, M.K., Johnson, D.P., 1995. New evidence for episodic post-glacial sea-level rise, central Great Barrier Reef, Australia. Marine Geology 127, 1-44.

Lewis, S.E., Wüst, R.A.J., Webster, J.M., Shields, G.A., 2008. Mid-late Holocene sea-level variability in eastern Australia. Terra Nova 20, 74-81.

Linsley, B.K., Ren, L., Dunbar, R.B., Howe, S.S., 2000. El Niño Southern Oscillation (ENSO) and decadal-scale climate variability at 10°N in the eastern Pacific from 1893 to 1994: A coral-based reconstruction from Clipperton Atoll. Paleoceanography 15, 322-335.

Lough, J.M., 2007. Tropical river flow and rainfall reconstructions from coral luminescence: Great Barrier Reef, Australia. Paleoceanography 22, PA2218.

Ludwig, K.R., 2003. Mathematical-statistical treatment of data and errors for Th-230/U geochronology. Uranium-Series Geochemistry 52, 631-656.

Madin, J.S., Connolly, S.R., 2006. Ecological consequences of major hydrodynamicdisturbances on coral reefs. Nature 444, 477–480.

Mastronuzzi, G., Sansò, P., 2000. Boulders transport by catastrophic waves along the Ionian coast of Apulia (southern Italy). Marine Geology 170, 93-103.

McAdoo, B.G., Ah-Leong, J.S., Bell, L., Ifopo, P., Ward, J., Lovell, E., Skelton, P., 2011. Coral reefs as buffers during the 2009 South Pacific tsunami, Upolu Island, Samoa. Earth-Science Reviews 107, 147-155.

McGowan, H.A., Marx, S.K., Denholm, J., Soderholm, J., Kamber, B.S., 2009. Reconstructing annual inflows to the headwater catchments of the Murray River, Australia, using the Pacific Decadal Oscillation. Geophysical Research Letters 36.

Moore, W.S., Krishnaswami, S., 1972. Coral growth rates using228Ra and210Pb. Earth and Planetary Science Letters 15, 187-190.

Nicholls, N., 1984. The Southern Oscillation, sea-surface-temperature, and interannual fluctuations in Australian tropical cyclone activity. Journal of Climatology 4, 661-670.

Nott, J., 1997. Extremely high-energy wave deposits inside the Great Barrier Reef, Australia: determining the cause—tsunami or tropical cyclone. Marine Geology 141, 193-207.

Nott, J., 2011. A 6000 year tropical cyclone record from Western Australia. Quaternary Science

Reviews 30, 713-722.

Nott, J., Forsyth, A., 2012. Punctuated global tropical cyclone activity over the past 5,000 years. Geophysical Research Letters 39.

Nott, J., Haig, J., Neil, H., Gillieson, D., 2007. Greater frequency variability of landfalling tropical cyclones at centennial compared to seasonal and decadal scales. Earth and Planetary Science Letters 255, 367-372.

Nott, J., Hayne, M., 2001. High frequency of 'super-cyclones' along the Great Barrier Reef over the past 5,000 years. Nature 413, 508-512.

Perry, C.T., Smithers, S.G., Kench, P.S., Pears, B., 2014.Impacts of Cyclone Yasi on nearshore, terrigenous sediment-dominated reefs of thecentral Great Barrier Reef, Australia. Geomorphology 222, 92-105.

Pezza, A.B., Simmonds, I., Renwick, J.A., 2007. Southern hemisphere cyclones and anticyclones: recent trends and links with decadal variability in the Pacific Ocean. International Journal of Climatology 27, 1403-1419.

Power, S., Casey, T., Folland, C., Colman, A., Mehta, V., 1999. Inter-decadal modulation of the impact of ENSO on Australia. Climate Dynamics 15, 319-324.

Ramsay, H.A., Leslie, L.M., 2008. The effects of complex terrain on severe landfalling tropical cyclone larry (2006) over northeast australia.Month Weather Review136, 4334–4354.

Robinson, L.F., Belshaw, N.S., Henderson, G.M., 2004. U and Th concentrations and isotope ratios in modern carbonates and waters from the Bahamas. Geochimica Et Cosmochimica Acta 68, 1777-1789.

Rodriguez-Ramirez, A., Grove, C.A., Zinke, J., Pandolfi, J.M., Zhao, J.-x., 2014. Coral Luminescence Identifies the Pacific Decadal Oscillation as a Primary Driver of River Runoff Variability Impacting the Southern Great Barrier Reef. Plos One 9, e84305.

Roff, G., Clark, T.R., Reymond, C.E., Zhao, J.-x., Feng, Y., McCook, L.J., Done, T.J., Pandolfi, J.M., 2013. Palaeoecological evidence of a historical collapse of corals at Pelorus Island, inshore Great Barrier Reef, following European settlement. Proceedings of the Royal Society B: Biological Sciences 280.

Scheffers, A., Kelletat, D., 2003. Sedimentologic and geomorphologic tsunami imprints worldwide—a review. Earth-Science Reviews 63, 83-92.

Scheffers, A., Scheffers, S., 2006. Documentation of the Impact of Hurricane Ivan on the Coastline of Bonaire (Netherlands Antilles). Journal of Coastal Research 22, 1437-1452.

Scheffers, S.R., Haviser, J., Browne, T., Scheffers, A., 2009. Tsunamis, hurricanes, the demise of coral reefs and shifts in prehistoric human populations in the Caribbean. Quaternary International 195, 69-87.

Shen, C.-C., Li, K.-S., Sieh, K., Natawidjaja, D., Cheng, H., Wang, X., Edwards, R.L., Lam, D.D., Hsieh, Y.-T., Fan, T.-Y., Meltzner, A.J., Taylor, F.W., Quinn, T.M., Chiang, H.-W., Kilbourne, K.H., 2008. Variation of initial ^{230}Th/^{232}Th and limits of high precision U–Th dating of shallow-water corals. Geochimica Et Cosmochimica Acta 72, 4201-4223.

Solow, A., Nicholls, N., 1990. The Relationship between the Southern Oscillation and Tropical Cyclone Frequency in the Australian Region. Journal of Climate 3, 1097-1101.

Viles, H.A., Goudie, A.S., 2003. Interannual, decadal and multidecadal scale climatic variability and geomorphology. Earth-Science Reviews 61, 105-131.

Walsh, K.J.E., Ryan, B.F., 2000. Tropical cyclone intensity increase near Australia as a result of climate change. Journal of Climate 13, 3029-3036.

Wang, C., Picaut, J., Understanding Enso Physics—A Review. In *Earth's Climate*, American Geophysical Union: 2013; pp 21-48.

Webster, P.J., Holland, G.J., Curry, J.A., Chang, H.R., 2005. Changes in Tropical Cyclone Number, Duration, and Intensity in a Warming Environment. Science 309, 1844-1846.

Yu, K.-F., Zhao, J.-X., Collerson, K.D., Shi, Q., Chen, T.-G., Wang, P.-X., Liu, T.-S., 2004. Storm cycles in the last millennium recorded in Yongshu Reef, southern South China Sea. Palaeogeography, Palaeoclimatology, Palaeoecology 210, 89-100.

Yu, K.-F., Zhao, J.-X., Wang, P.-X., Shi, Q., Meng, Q.-S., Collerson, K.D., Liu, T.-S., 2006. High-precision TIMS U-series and AMS ^{14}C dating of a coral reef lagoon sediment core from southern South China Sea. Quaternary Science Reviews 25, 2420-2430.

Yu, K., Zhao, J.-x., Shi, Q., Price, G.J., 2012a. Recent massive coral mortality events in the South China Sea: Was global warming and ENSO variability responsible? Chemical Geology 320–321, 54-65.

Yu, K., Zhao, J., Roff, G., Lybolt, M., Feng, Y., Clark, T., Li, S., 2012b. High-precision U-series ages of transported coral blocks on Heron Reef (southern Great Barrier Reef) and storm activity during the past century. Palaeogeography, Palaeoclimatology, Palaeoecology 337–338, 23-36.

Yu, K.F., Zhao, J.X., 2010. U-series dates of Great Barrier Reef corals suggest at least +0.7 m sea level similar to 7000 years ago. Holocene 20, 161-168.

Zhao, J.-x., Neil, D.T., Feng, Y.-x., Yu, K.-f., Pandolfi, J.M., 2009a. High-precision U-series dating of very young cyclone-transported coral reef blocks from Heron and Wistari reefs, southern Great Barrier Reef, Australia. Quaternary International 195, 122-127.

Zhao, J.-x., Yu, K.-f., Feng, Y.-x., 2009b. High-precision $^{238}U–^{234}U–^{230}Th$ disequilibrium dating of the recent past: a review. Quaternary Geochronology 4, 423-433.

Collected figure captions

Figure 1. Map showing the location of the Frankland Islands group and the distribution of coral block samples on the Frankland Islands, northern Great Barrier Reef.

Figure 2. Photographs showing transported coral blocks on the Frankland Islands: (a) NI-SB-H6-06, massive coral (*Favia*); (b) NI-SB-H6-07, massive coral *Platygyra*; (c)NI-SB-H6-04, massive coral (*Goniastrea*); (d)NI-SB-001, massive *Goniastrea* block with well-preserved surface.

Figure 3. ^{230}Th/^{232}Th vs. ^{238}U/^{232}Th isochron diagram defined by 18 sub-samples from 6 transported coral blocks collected on the Frankland Islands, northern GBR. Insert figure shows the isochron-inferred initial ^{230}Th/^{232}Th ratios representing the Th isotopic composition of the detrital component (average 0.64).

Figure 4. Diagrams showing: A. Global Sea Surface Temperature (from http://www.bom.gov.au/climate/change/?ref=ftr#tabs=Tracker&tracker=timeseries&tQ%5Bgraph%5D=sst&tQ%5Barea%5D=qld&tQ%5Bseason%5D=0112&tQ%5Bave_yr%5D=0); B. Summer Rainfall (from the book of "Queensland Rainfall Data"); C. PDO index since 1900AD, http://jisao.washington.edu/pdo/PDO.latest; D. cyclones crossing within 200 km from Frankland Reefs between 1900 and 2005AD (from http://www.bom.gov.au) for comparison with the surface (mortality) ages of transported coral blocks dated to this period; E. Relative probability plot defined by the mortality ages of

the transported coral blocks dated between 1900 and 2005AD; F. Relative

probability plot defined by the mortality ages of all the dated transported coral

blocks; G. PDO index in the last millennium (from

ftp://ftp.ncdc.noaa.gov/pub/data/paleo/treering/reconstructions/pdo-macdonald2

005.txt)

Figure 5. The surface mortality ages of the transported coral blocks on Normanby

Island, northern GBR show a decreasing age trend from shore to reef edge

(from 758.4±3.7AD to 1988.3±1.6 AD).
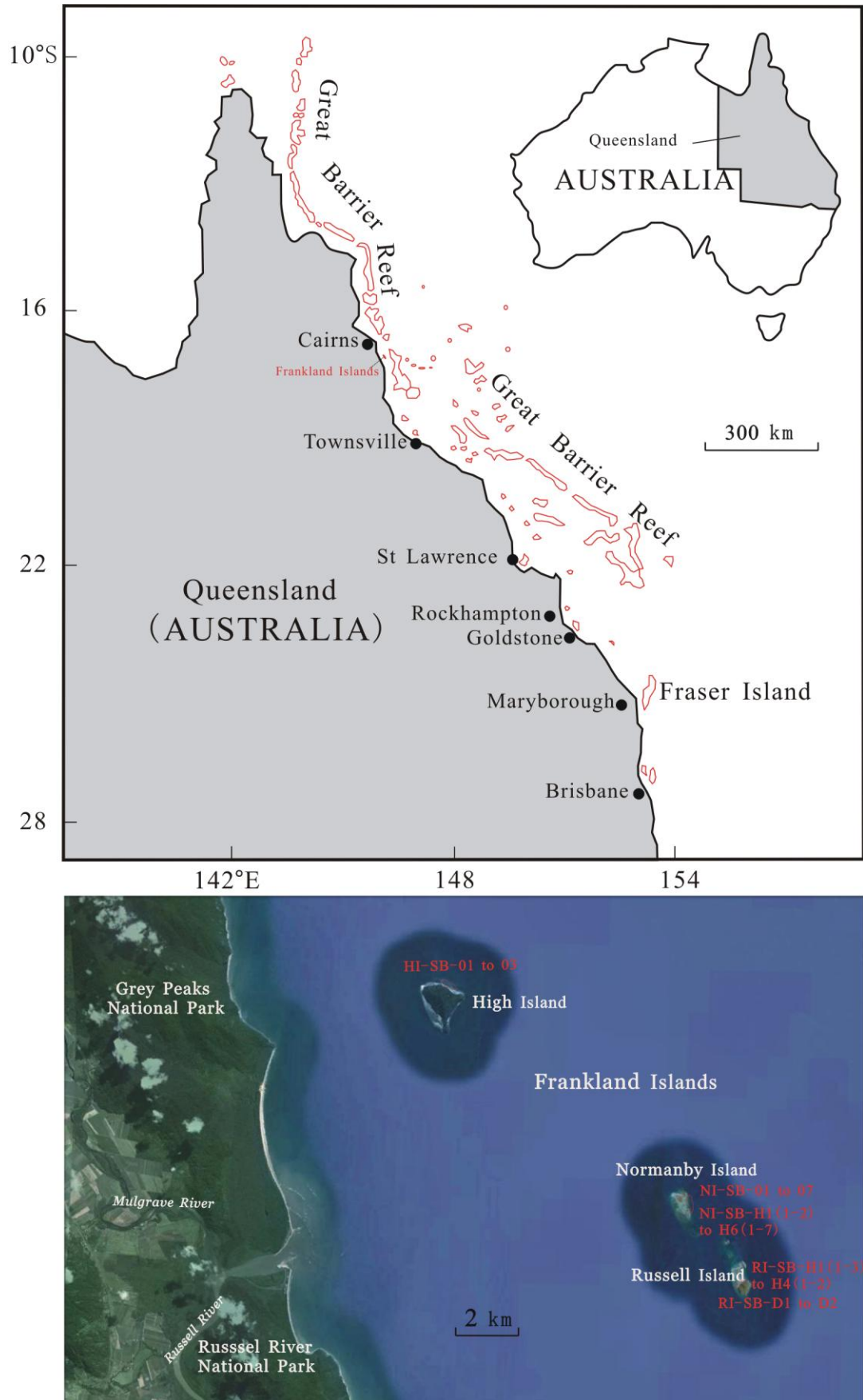
Figure 1

Figure 2
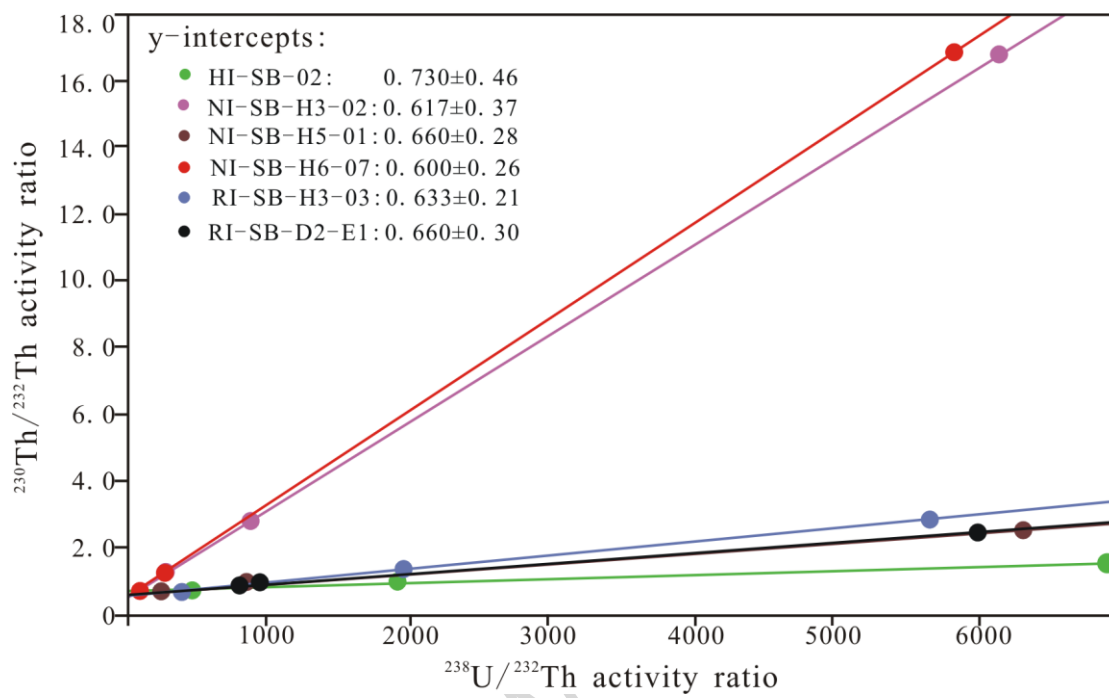
Figure 3
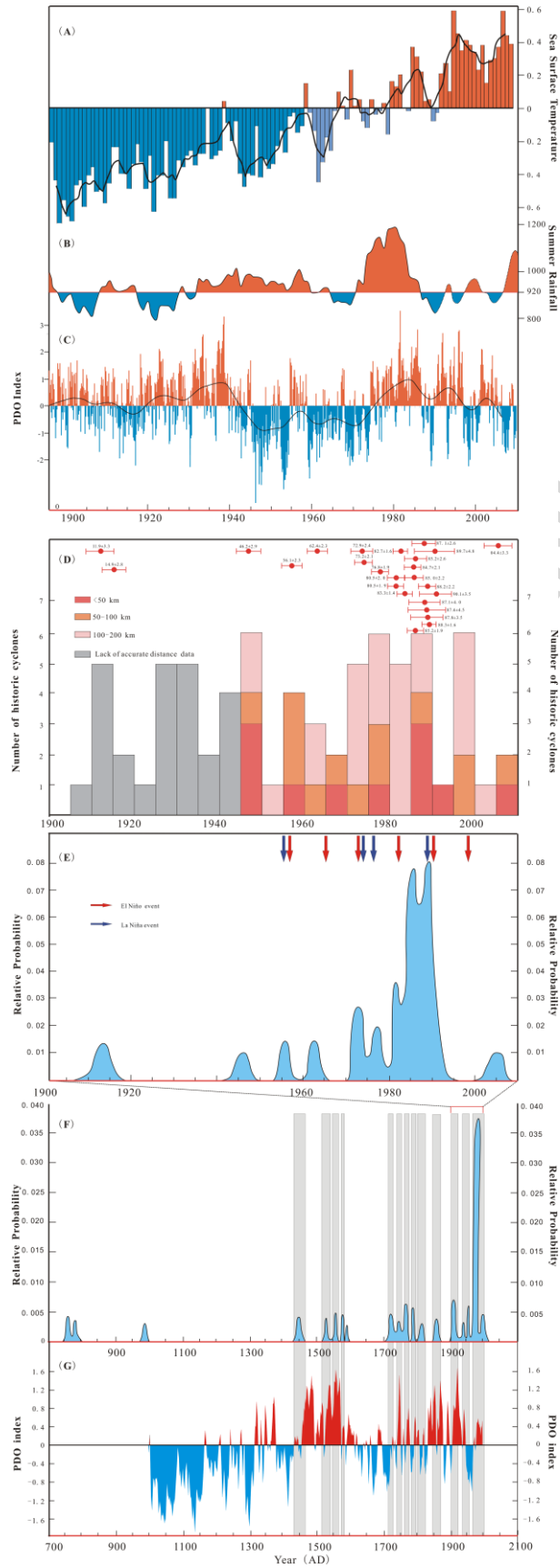
Figure 4
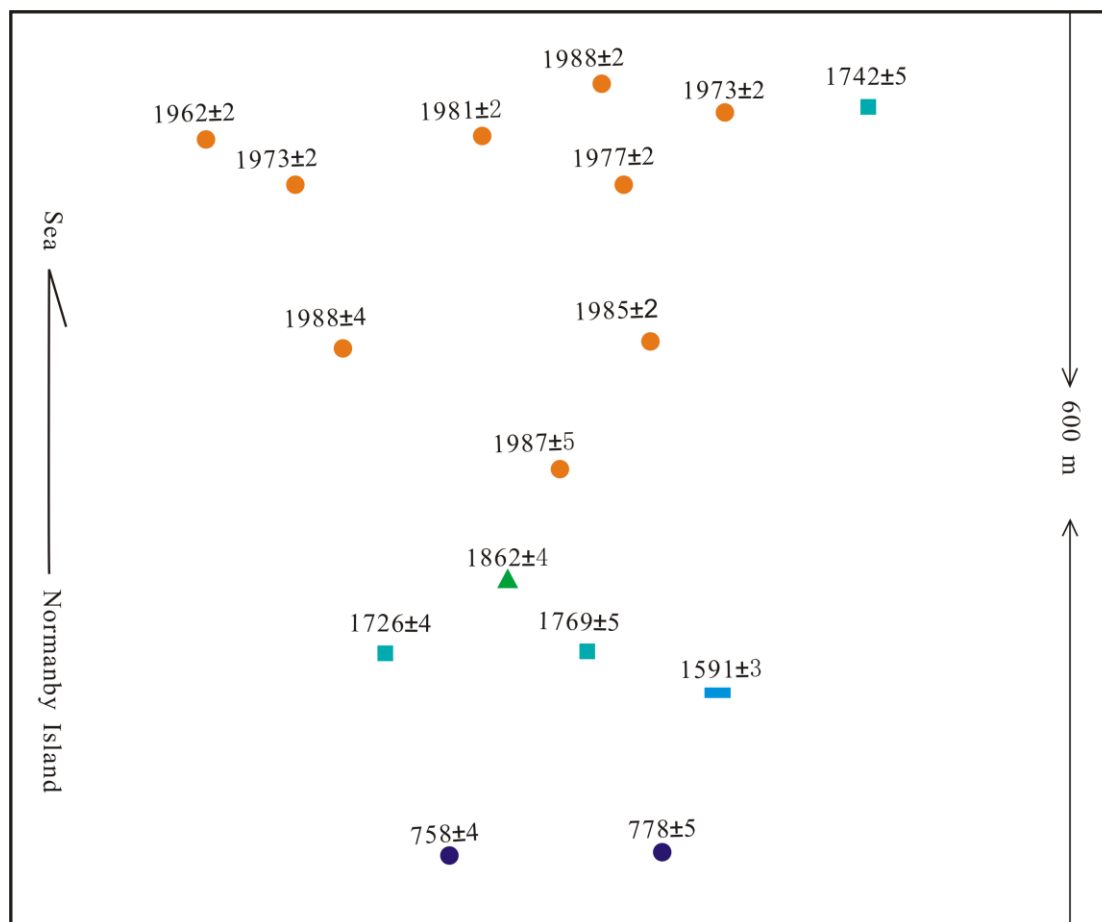
Figure 5

Collected table captions

Table 1. MC-ICP-MS [230]Th ages for storm-transported corals collected from the Frankland Islands, northern Great Barrier Reef**.**

Table 2. MC-ICP-MS [230]Th data for uncleaned, normal-cleaned and ultra-cleaned storm-transported coral blocks collected from the Frankland Islands, northern Great Barrier Reef**.**

Table 3. The potentially responsible storms/cyclones from 1941AD to 2005 AD within 200 km of the Frankland Islands, northern Great Barrier Reef

Table 1. MC-ICP-MS [230]Th ages for storm-transported corals collected from the Frankland Islands, northern Great Barrier Reef.

| Sample Name	Block Size (m³)	Coral Family Name	U (ppm)	[232]Th (ppb)	([230]Th/[232]Th)meas	([230]Th/[238]U)	([234]U/[238]U)	Uncorr. [230]Th age (a)	Corr. [230]Th age (a)	Time of chemistry	Corr. [230]Th Age (AD)	Annual bands	Mortality yr in AD
HI-SB-01	0.12	*Poritidae*	2.6412±0.0013	0.7838±0.0009	111.1±0.39	0.010868±0.000037	1.1459±0.0009	1040.4±3.6	1029.4±4.3	2013.11	983.7±4.3	1	985.2±4.8
HI-SB-02	1.05	*Poritidae*	2.6630±0.0014	1.1614±0.0013	1.69±0.03	0.000243±0.000005	1.1438±0.0010	23.2±0.5	9.5±2.8	2013.41	2003.9±2.8	0	2004.4±3.3
HI-SB-03	1.20	*Poritidae*	2.3665±0.0012	1.8318±0.0017	1.90±0.03	0.000486±0.000009	1.1440±0.0008	46.4±0. 8	25.2±4.3	2013.41	1988.2±4.3	1	1989.7±4.8
NI-SB-001/1	0.24	*Faviidae*	2.7050±0.0014	0.2647±0.0006	24.85±0.63	0.000802±0.000020	1.1488±0.0010	76.2±1.9	69.4±2.4	2013.04	1943.7±2.4	2	1946.2±2.9
NI-SB-001B/1	0.20	*Faviidae*	2.4575±0.0011	1.3824±0.0013	12.14±0.18	0.002251±0.000033	1.1485±0.0009	214.2±3.1	197.6±4.6	2013.04	1815.4±4.6	1	1816.9±5.1
NI-SB-002/1	0.54	*Faviidae*	4.2450±0.0025	0.8721±0.0019	5.24±0.13	0.000355±0.000009	1.1419±0.0008	33.9±0.8	26.7±1.7	2013.41	1986.7±1.7	1	1988.2±2.2
NI-SB-002R02-03/1	0.42	*Acroporidae*	3.1867±0.0012	0.4195±0.0008	111.19±0.70	0.004824±0.000029	1.1456±0.0010	460.7±2.8	453.9±3.1	2013.04	1559.1±3.1	1	1560.6±3.6
NI-SB-003-OG/1	0.28	*Poritidae*	2.2341±0.0007	0.1308±0.0005	57.53±0.97	0.001110±0.000018	1.1469±0.0012	105.7±1.7	98.6±2.3	2013.04	1914.4±2.3	0	1914.9±2.8
NI-SB-004/1	0.48	*Poritidae*	3.1507±0.0010	1.8619±0.0016	15.02±0.19	0.002925±0.000037	1.1474±0.0010	262.7±4.8	262.7±4.8	2013.04	1750.4±4.8	1	1751.9±5.3
NI-SB-005/1	0.56	*Faviidae*	2.2842±0.0013	0.0401±0.0003	117.3±2.5	0.000678±0.000014	1.1470±0.0011	64.5±1.3	58.4±1.8	2013.04	1954.6±1.8	1	1956.1±2.3
NI-SB-006/1	1.12	*Faviidae*	3.0724±0.0011	0.4339±0.0005	24.75±0.54	0.001152±0.000025	1.1469±0.0008	109.7±2.4	102.6±2.8	2013.04	1910.4±2.8	1	1911.9±3.3
NI-SB-007/1	0.24	*Faviidae*	2.5471±0.0012	0.0647±0.0003	44.5±1.3	0.000373±0.000011	1.1468±0.0010	35.5±1.0	29.8±1.6	2013.04	1983.2±1.6	1	1984.7±2.1
NI-SB-H1-01	0.33	*Faviidae*	2.4319±0.0011	0.1375±0.0003	707.4±2.3	0.013181±0.000029	1.1461±0.0010	1262.8±3.0	1256.3±3.2	2013.11	756.9±3.2	1	758.4±3.7
NI-SB-H1-02	0.28	*Acroporidae*	3.4419±0.0015	1.1078±0.0016	122.64±0.41	0.013009±0.000040	1.1464±0.0008	1246.0±3.9	1235.7±4.4	2013.11	777.4±4.4	0	777.9±4.9
NI-SB-H3-01	0.72	*Faviidae*	2.9536±0.0012	0.2416±0.0004	167.0±1.0	0.004503±0.000026	1.1470±0.0010	429.5±2.5	423.4±2.8	2013.11	1589.7±2.8	1	1591.2±3.3
NI-SB-H3-02	0.28	*Faviidae*	2.1688±0.0009	1.0734±0.0013	16.72±0.15	0.002728±0.000025	1.1442±0.0011	260.7±2.4	244.6±4.0	2013.41	1768.8±4.0	0	1769.3±4.5
NI-SB-H3-03	0.36	*Faviidae*	3.5501±0.0018	1.9760±0.0025	17.17±0.12	0.00315±0.000022	1.1477±0.0007	300.1±2.1	288.8±3.1	2013.08	1724.3±3.1	1	1725.8±3.6
NI-SB-H3-04	0.28	*Acroporidae*	3.3091±0.0012	1.9179±0.0028	9.17±0.10	0.001752±0.000019	1.1466±0.0007	167.0±1.8	151.4±3.6	2013.11	1861.7±3.6	0	1862.2±4.1
NI-SB-H4-01	0.84	*Faviidae*	3.2515±0.0017	2.4387±0.0027	1.92±0.05	0.000476±0.000011	1.1451±0.0009	45.4±1.1	26.2±4.0	2013.11	1986.9±4.0	0	1987.4±4.5
NI-SB-H5-01	0.22	*Faviidae*	2.7756±0.0017	1.3488±0.0015	2.66±0.04	0.000426±0.000006	1.1421±0.0008	40.7±0.6	26.1±3.0	2013.41	1987.3±3.0	0	1987.8±3.5
NI-SB-H5-02	0.16	*Acroporidae*	3.7310±0.0023	0.5026±0.0010	8.26±0.13	0.000367±0.000006	1.1450±0.0011	35.0±0.5	28.7±1.4	2013.41	1984.7±1.4	0	1985.2±1.9
NI-SB-H6-01	0.15	*Faviidae*	2.5027±0.0015	0.3869±0.0006	10.13±0.17	0.000516±0.000009	1.1489±0.0010	49.1±0.8	40.7±1.9	2013.11	1972.4±1.9	0	1972.9±2.4
NI-SB-H6-02	0.14	*Faviidae*	3.8152±0.0021	0.4403±0.0005	11.03±0.26	0.000419±0.000010	1.1486±0.0010	39.9±0.9	34.1±1.5	2013.11	1979.0±1.5	1	1980.5±2.0
NI-SB-H6-03	0.64	*Faviidae*	3.6977±0.0023	0.2147±0.0003	16.90±0.33	0.000323±0.000006	1.1448±0.0008	30.8±0.6	26.1±1.1	2013.41	1987.3±1.1	0.5	1988.3±1.6
NI-SB-H6-04	0.44	*Faviidae*	2.4587±0.0009	0.0725±0.0004	47.31±0.87	0.000460±0.000008	1.1462±0.0009	43.8±0.8	37.8±1.4	2013.11	1975.3±1.4	1	1976.8±1.9
NI-SB-H6-05	0.32	*Faviidae*	2.3833±0.0006	0.0450±0.0002	98.1±2.4	0.000610±0.000014	1.1478±0.0008	58.1±1.4	52.2±1.8	2013.11	1960.9±1.8	1	1962.4±2.3
NI-SB-H6-06	1.32	*Faviidae*	2.4826±0.0013	0.1106±0.0003	33.72±0.72	0.000495±0.000011	1.1472±0.0009	47.1±1.0	40.9±1.6	2013.11	1972.2±1.6	0.5	1973.2±2.1
NI-SB-H6-07	1.08	*Faviidae*	2.2615±0.0012	1.2280±0.0017	16.90±0.18	0.003025±0.000033	1.1463±0.0009	288.5±3.1	271.7±4.6	2013.41	1741.7±4.6	0	1742.2±5.1
RI-SB-H1-01	0.14	*Acroporidae*	3.2844±0.0012	0.3112±0.0007	78.35±0.94	0.002447±0.000029	1.1467±0.0006	233.2±2.8	227.3±3.0	2013.11	1785.8±3.0	0	1786.3±3.5

Sample Name	Block Size (m³)	Coral Family	U (ppm)	²³²Th (ppb)	(²³⁰Th/²³²Th)meas	(²³⁰Th/²³⁸U)	(²³⁴U/²³⁸U)	Uncorr. ²³⁰Th age (a)	Corr. ²³⁰Th age (a)	Time of chemistry	Corr. ²³⁰Th Age (AD)	Annual bands	Mortality yr in AD
RI-SB-H1-02	0.14	*Acroporidae*	3.5556±0.0024	0.1357±0.0006	209.6±2.6	0.002635±0.000031	1.1485±0.0009	250.8±2.9	246.4±3.1	2013.11	1766.7±3.1	0	1767.2±3.6
RI-SB-H1-03	0.12	*Acroporidae*	2.4689±0.0012	0.3125±0.0004	123.18±0.81	0.005139±0.000033	1.1451±0.0009	491.1±3.2	483.2±3.6	2013.11	1530.0±3.3	0	1530.5±3.8
RI-SB-H2-01	0.16	*Acroporidae*	3.4475±0.0019	0.7563±0.0017	64.05±0.42	0.004631±0.000029	1.1463±0.0010	442.0±2.8	433.8±3.2	2013.11	1579.3±3.2	1	1580.8±3.7
RI-SB-H2-02	0.15	*Acroporidae*	3.8501±0.0027	2.6873±0.0022	26.27±0.14	0.006042±0.000032	1.1468±0.0010	576.8±3.1	559.3±4.7	2013.11	1453.8±4.7	1	1455.3±5.2
RI-SB-H2-03	0.18	*Acroporidae*	4.0184±0.0020	1.0911±0.0030	66.99±0.36	0.005995±0.000028	1.1469±0.0009	572.2±2.7	563.4±3.2	2013.11	1449.7±3.2	0	1450.2±3.7
RI-SB-H3-01	0.18	*Faviidae*	3.2709±0.0012	0.8690±0.0023	4.30±0.10	0.000377±0.000009	1.1463±0.0008	35.9±0.8	26.5±2.1	2013.11	1986.6±2.1	0	1987.1±2.6
RI-SB-H3-02	0.12	*Acroporidae*	2.3974±0.0011	0.1342±0.0005	19.99±0.88	0.000369±0.000016	1.1477±0.001	35.1±1.5	28.5±2.1	2013.11	1984.7±2.1	0	1985.2±2.6
RI-SB-H3-03	0.12	*Acroporidae*	1.9940±0.0011	1.0521±0.0012	2.66±0.04	0.000462±0.000007	1.1459±0.0008	44.0±0.7	26.8±3.5	2013.41	1986.6±3.5	0	1987.1±4.0
RI-SB-H4-01	0.23	*Faviidae*	2.3401±0.0015	0.0963±0.0003	27.91±0.79	0.000378±0.000011	1.1458±0.0009	36.1±1.0	29.6±1.7	2013.11	1983.5±1.7	1	1985.0±2.2
RI-SB-H4-02	0.18	*Faviidae*	2.3474±0.0016	0.1120±0.0003	27.53±0.39	0.000433±0.000006	1.1488±0.0012	41.1±0.6	34.6±1.4	2013.11	1978.5±1.4	1.5	1980.5±1.9
RI-SB-D1-E1	1.80	*Faviidae*	2.6001±0.0009	0.0560±0.0005	46.9±1.7	0.000333±0.000012	1.1470±0.0010	31.7±1.1	26.2±1.6	2013.11	1982.2±1.1	0	1982.7±1.6
RI-SB-D1-E2	1.80	*Faviidae*	2.3872±0.0012	0.0521±0.0003	45.6±1.3	0.000328±0.000009	1.1466±0.0009	31.2±0.9	25.3±1.5	2013.11	1982.8±0.9	0	1983.3±1.4
RI-SB-D2-E1	1.36	*Faviidae*	2.8839±0.0016	1.4643±0.0018	2.48±0.04	0.000415±0.000006	1.1457±0.0010	39.6±0.6	24.8±3.0	2013.41	1988.6±3.0	1	1990.1±3.5

Note: Ratios in parentheses are activity ratios calculated from atomic ratios using decay constants of Cheng et al. (2000). All values have been corrected for laboratory procedural lanks. All errors reported in this table are quoted as 2σ. Uncorrected ²³⁰Th age was calculated using Isoplot/EX 3.0 program (Ludwig, 2003b). Assuming that post-mortality erosion was minimal, the exact time of the coral mortality was calculated by adding the number of growth bands above the sampling location to the U-Th age. Considering the uncertainties in sampling location, ±0.5 year was added to the mortality age uncertainties. The number of annual bands was identified from the sampling location to the mortality surface.

Table 2. MC-ICP-MS ²³⁰Th data for uncleaned, normal-cleaned and ultra-cleaned storm-transported coral blocks collected from the Frankland Islands, northern Great Barrier Reef.

Sample Name	Block Size (m³)	Coral Family	U (ppm)	²³²Th (ppb)	(²³⁰Th/²³²Th)meas	(²³⁰Th/²³⁸U)	(²³⁴U/²³⁸U)	Uncorr. ²³⁰Th age (a)	Corr. ²³⁰Th age (a)	Time of chemistry	Corr. ²³⁰Th Age (AD)	Annual bands	Mortality yr in AD
HI-SB-02(C)	1.05	*Poritidae*	2.5806±0.0014	4.0935±0.0047	1.03±0.02	0.000537±0.000012	1.1485±0.0014	51.1±1.2	14.2±7.6	2013.11	1999.0±7.6	0	1999.5±8.1
HI-SB-02 (E)	1.05	*Poritidae*	2.6630±0.0014	1.1614±0.0013	1.69±0.03	0.000243±0.000005	1.1438±0.0010	23.2±0.5	9.5±2.8	2013.41	2003.9±2.8	0	2004.4±3.3
HI-SB-02 (U)	1.05	*Poritidae*	2.7696±0.0021	20.804±0.081	0.76±0.01	0.001876±0.000022	1.1464±0.0013	178.8±2.1	23±31	2013.41	1990±31	0	1991±32
NI-SB-H3-02(C)	0.28	*Faviidae*	2.9807±0.0015	10.601±0.015	2.83±0.03	0.003317±0.000034	1.1477±0.0011	316.1±3.3	240±16	2013.11	1773±16	0	1773±16
NI-SB-H3-02 (E)	0.28	*Faviidae*	2.1688±0.0009	1.0734±0.0013	16.72±0.15	0.002728±0.000025	1.1442±0.0011	260.7±2.4	244.6±4.0	2013.41	1768.8±4.0	0	1769.3±4.5
NI-SB-H3-02 (U)	0.28	*Faviidae*	2.9894±0.0014	36.005±0.088	1.30±0.01	0.005173±0.000045	1.1466±0.0008	493.7±4.3	247±50	2013.41	1766±50	0	1767±50

NI-SB-H5-01(C)	0.22	*Faviidae*	3.4720±0.0015	13.275±0.010	0.93±0.01	0.001177±0.000018	1.1486±0.0009	111.9±1.7	31±16	2013.11	1982±16	0	1982±17
NI-SB-H5-01(E)	0.22	*Faviidae*	2.7756±0.0017	1.3488±0.0015	2.66±0.04	0.000426±0.000006	1.1421±0.0008	40.7±0.6	26.1±3.0	2013.41	1987.3±3.0	0	1987.8±3.5
NI-SB-H5-01(U)	0.22	*Faviidae*	3.3891±0.0019	58.372±0.061	0.70±0.01	0.003950±0.000042	1.1459±0.0012	377.0±4.1	26±71	2013.41	1987±71	0	1988±71
NI-SB-H6-07(C)	1.08	*Faviidae*	3.0163±0.0014	34.310±0.086	1.36±0.01	0.005101±0.000035	1.1482±0.0008	486.2±3.4	253±47	2013.11	1760±47	0	1760±47
NI-SB-H6-07(E)	1.08	*Faviidae*	2.2615±0.0012	1.2280±0.0017	16.9±0.18	0.003025±0.000033	1.1463±0.0009	288.5±3.1	271.7±4.6	2013.41	1741.7±4.6	0	1742.2±5.1
NI-SB-H6-07(U)	1.08	*Faviidae*	3.1100±0.0022	144.28±0.80	0.81±0.01	0.012438±0.000100	1.1452±0.0015	1192.3±9.8	251±190	2013.41	1762±190	0	1762±190
RI-SB-H3-03(C)	0.12	*Acroporidae*	2.5417±0.0013	4.0155±0.012	1.33±0.02	0.000690±0.000010	1.146±0.0009	65.8±1.0	28.8±7.5	2013.11	1984.3±7.5	0	1984.8±8.0
RI-SB-H3-03(E)	0.12	*Acroporidae*	1.9940±0.0011	1.0521±0.0012	2.66±0.04	0.000462±0.000007	1.1459±0.0008	44.0±0.7	26.8±3.5	2013.41	1986.6±3.5	0	1987.1±4.0
RI-SB-H3-03(U)	0.12	*Acroporidae*	2.9209±0.0016	37.705±0.078	0.71±0.01	0.003001±0.000027	1.1458±0.0011	286.4±2.6	22±53	2013.41	1991±53	0	1992±54
RI-SB-D2-E1(C)	1.36	*Faviidae*	2.6470±0.0014	9.6071±0.0088	0.90±0.02	0.001075±0.000024	1.1482±0.0009	102.3±2.3	24±16	2013.11	1989±16	1	1990±16
RI-SB-D2-E1(E)	1.36	*Faviidae*	2.8839±0.0016	1.4643±0.0018	2.48±0.04	0.000415±0.000006	1.1457±0.0010	39.6±0.6	24.8±30	2013.41	1988.6±3.0	1	1990.1±3.5
RI-SB-D2-E1(U)	1.36	*Faviidae*	2.9165±0.0017	9.1709±0.023	0.98±0.02	0.001012±0.000016	1.1449±0.0012	96.6±1.6	29±14	2013.41	1985±14	1	198±14

Note: Ratios in parentheses are activity ratios calculated from atomic ratios using decay constants of Cheng et al. (2000). All values have been corrected for laboratory procedural lanks. All errors reported in this table are quoted as 2σ.

[a]C, E, U are replicate samples taken from within the same growth band. C means common-cleaned subsample; E means enhance-cleaned subsample; U means uncleaned sample.

Table 3. The potentially responsible storms/cyclones from 1941AD to 2005 AD within

200 km of the Frankland Islands, northern Great Barrier Reef

Period	0-50km	50-100 km	100-200 km
2001-2007	Larry: 14-20/03/2006 (5)	Jim: 23-30/1/2006 (3) Abigail: 24/2-8/3/2001 (3)	
1991-2000		Justin: 6-23/3/1997 (3) Joy: 18-27/12/1990 (4) Rona-Frank: 9/12/1999 (3)	Steve: 27/2-11/3/2000 (3) Gillian: 10-12/2/1997 (1) Tessi: 1-2/4/2000 (2)
1981-1990	Felicity: 13-20/12/1989 (2) Ivor: 16-26/3/1990 (4) Winifred:27/1-5/2/1986 (3)	Vernon: 21-24/1/1986 (1)	Pierre: 18-24/2/1985 (1); Freda: 24/2-7/3/1981 (2) Des:14-23/1/1983(2); Ingrid:20-25/2/1984 (5); Dominic:4-14/4/1982(2); Delilah:28/12/1988-01/1/1989 (2)
1971-1980	Dawn: 3-6/3/1976 (1)	Otto: 6-10/3/1977 (2) Keith: 29-31/1/1977 (1) Gertie: 10-16/2/1971 (2)	Kerry:12/2-04/3/1979(4); Hal:6-11/4/1978(unknown) Una:14-20/12/73(unknown); Gloria:15-19/1/1975 (3) Yvonne: 8-11/2/1974 (1); Althea: 19-29/12/1971 (4) Peter: 29/12/78-3/1/1979 (3)
1961-1970	Judy:25/1-5/2/1965 (unknown)	Elaine: 13-19/3/1967 (unknown) Flora: 30/11-08/12/1964 (unknown)	Unnamed#13:02-08/3/1961(unknown);Bridget:23-26/1/1969 (unknown); Unnamed#3: 2-6/1/1961 (unknown)
1951-1960	Unnamed#7:01-18/3/1955 (unknown) Bertha:4-22/1/1959 (unknown) Unnamed#1:6-12/2/1956 (unknown)	Unnamed#2:24-31/12/1959 (unknown)	Agnes: 23/2-11/3/1956 (unknown) Unnamed #10: 06-12/2/1956 (unknown)
1941-1950	Unnamed#4:6-11/2/1946 (unknown) Unnamed#3:10-15/1/1948 (unknown) Unnamed#6:27/2-03/3/1946 (unknown)	Unnamed#5:15-21/2/1942(unknown) Unnamed#1:1-14/2/1947 (unknown)	Unnamed#2:12-16/1/1950(unknown);Unnamed#7:4-11/3/1950 (unknown);Unnamed#8: 15-21/12/1942 (unknown); Unnamed #9: 29/1-2/2/1945 (unknown)

The style of cyclone is this table: Cyclone Name: time (Category). The categories of cyclones are indentified with the data from Wikipedia, Australian Government Bureau of Meteorology and http://australiancyclones.com/Cyclone-List.php.

Highlights

● We present the first palaeostorm reconstruction using U-Th dating of inshore blocks

● 17 additional storm events prior to 1850's were identified

● The storm activities were modulated by the multi-decadal PDO index

● There is a decreasing age trend from shore to reef edge in mortality age distribution